



## OPEN ACCESS

## EDITED BY

Madhav Bhatia,  
University of Otago, New Zealand

## REVIEWED BY

Hua Ren,  
East China Normal University, China  
Veeresh Kumar Sali,  
The University of Iowa, United States

## \*CORRESPONDENCE

Gang Li

✉ gang.lihndx@163.com

Pengxiang Guo

✉ gpxtcm@163.com

†These authors have contributed  
equally to this work and share  
first authorship

RECEIVED 03 January 2024

ACCEPTED 29 February 2024

PUBLISHED 15 March 2024

## CITATION

Li G, Yan K, Zhang W, Pan H and Guo P  
(2024) ARDS and aging: TYMS emerges as a  
promising biomarker and therapeutic target.  
*Front. Immunol.* 15:1365206.  
doi: 10.3389/fimmu.2024.1365206

## COPYRIGHT

© 2024 Li, Yan, Zhang, Pan and Guo. This is an  
open-access article distributed under the terms  
of the [Creative Commons Attribution License  
\(CC BY\)](https://creativecommons.org/licenses/by/4.0/). The use, distribution or reproduction  
in other forums is permitted, provided the  
original author(s) and the copyright owner(s)  
are credited and that the original publication  
in this journal is cited, in accordance with  
accepted academic practice. No use,  
distribution or reproduction is permitted  
which does not comply with these terms.

# ARDS and aging: TYMS emerges as a promising biomarker and therapeutic target

Gang Li<sup>1\*†</sup>, Ke Yan<sup>2†</sup>, Wanyi Zhang<sup>1</sup>, Haiyan Pan<sup>1</sup>  
and Pengxiang Guo<sup>3\*</sup>

<sup>1</sup>Department of Emergency Medicine, The Third Affiliated Hospital of Zhejiang Chinese Medical University, Hangzhou, Zhejiang, China, <sup>2</sup>School of Life Sciences, Beijing University of Chinese Medicine, Beijing, China, <sup>3</sup>Department of Pharmacology of Chinese Materia Medica, School of Traditional Chinese Pharmacy, China Pharmaceutical University, Nanjing, China

**Background:** Acute Respiratory Distress Syndrome (ARDS) is a common condition in the intensive care unit (ICU) with a high mortality rate, yet the diagnosis rate remains low. Recent studies have increasingly highlighted the role of aging in the occurrence and progression of ARDS. This study is committed to investigating the pathogenic mechanisms of cellular and genetic changes in elderly ARDS patients, providing theoretical support for the precise treatment of ARDS.

**Methods:** Gene expression profiles for control and ARDS samples were obtained from the Gene Expression Omnibus (GEO) database, while aging-related genes (ARGs) were sourced from the Human Aging Genomic Resources (HAGR) database. Differentially expressed genes (DEGs) were subjected to functional enrichment analysis to understand their roles in ARDS and aging. The Weighted Gene Co-expression Network Analysis (WGCNA) and machine learning pinpointed key modules and marker genes, with ROC curves illustrating their significance. The expression of four ARDS-ARDEGs was validated in lung samples from aged mice with ARDS using qRT-PCR. Gene set enrichment analysis (GSEA) investigated the signaling pathways and immune cell infiltration associated with TYMS expression. Single-nucleus RNA sequencing (snRNA-Seq) explored gene-level differences among cells to investigate intercellular communication during ARDS onset and progression.

**Results:** ARDEGs are involved in cellular responses to DNA damage stimuli, inflammatory reactions, and cellular senescence pathways. The MEMagenta module exhibited a significant correlation with elderly ARDS patients. The LASSO, RRF, and XGBoost algorithms were employed to screen for signature genes, including CKAP2, P2RY14, RBP2, and TYMS. Further validation emphasized the potential role of TYMS in the onset and progression of ARDS. Immune cell infiltration indicated differential proportion and correlations with TYMS expression. SnRNA-Seq and cell-cell communication analysis revealed that TYMS is highly expressed in endothelial cells, and the SEMA3 signaling pathway primarily mediates cell communication between endothelial cells and other cells.

**Conclusion:** Endothelial cell damage associated with aging could contribute to ARDS progression by triggering inflammation. TYMS emerges as a promising diagnostic biomarker and potential therapeutic target for ARDS.

#### KEYWORDS

ARDS, aging, TYMS, WGCNA, machine learning, immune infiltration, snRNA-seq

## 1 Introduction

Acute Respiratory Distress Syndrome (ARDS) represents a life-threatening manifestation of severe respiratory failure that can occur in any condition or disease that causes lung injury (1). The pathological changes in ARDS are characterized by diffuse alveolar damage, including damage to alveolar epithelial and pulmonary capillary endothelial cells, inflammation and infiltration of immune cells, widening of interstitial edema, protein-rich edema fluid in the alveoli, fibrous protein deposition, formation of transparent membranes, and microthrombosis (2). These changes lead to dysregulation of the ventilation/perfusion (V/Q) ratio, impaired gas exchange, a significant increase in intrapulmonary shunting, decreased lung compliance, reduced lung volume (baby lung), and ultimately acute hypoxemic respiratory failure (3). The mortality rate of ARDS is as high as 40% (4), making it one of the main reasons for patients to be transferred to the ICU (5). Based on statistics, the incidence rate of ARDS is several tens of cases per 100,000 person-years (6). Numerous studies have shown that elderly patients account for a high proportion of ARDS patients, and age is a significant risk factor affecting the development and prognosis of ARDS (7). Currently, the diagnosis of ARDS mainly relies on clinical manifestations, but the problem of missed diagnosis and delayed diagnosis remains unresolved. Therefore, studying the molecular biological mechanisms of ARDS and identifying potential biomarkers is of great significance for early recognition, diagnosis, and assessment of the severity and prognosis of ARDS.

Increasing evidence suggests that the pathogenesis of ARDS involves multiple biological functions, including inflammatory response (8), oxidative stress (9), apoptosis (10, 11), and endoplasmic reticulum autophagy (12). Amidst these factors, aging is pivotal in the genesis and advancement of ARDS. Aging is a complex and multidimensional process that leads to widespread organ dysfunction (13) and various age-related diseases (14), such as neurodegenerative disorders, diabetes, idiopathic pulmonary fibrosis, etc. (15). DNA damage serves as a primary catalyst for aging, whereas DNA repair acts as a pivotal determinant of aging. Additionally, deficiencies in DNA repair can accelerate the progression of various age-related diseases (16). Lung aging is associated with molecular and physiological changes that result in altered lung function, impaired lung remodeling and regeneration, and increased susceptibility to acute and chronic lung diseases (17). Older patients with sepsis have worse outcomes, which may be related to the decline in immune system

function and changes in the pulmonary vascular system in the elderly (18, 19). Immune cell activation is a major mediator of ARDS inflammation, and immunosenescence may affect the pathogenesis and prognosis of elderly ARDS subgroups (20). A cross-age study of ARDS patients showed a correlation between age and neutrophil biomarker myeloperoxidase (MPO) in bronchoalveolar lavage fluid (BALF) (21). Compared with younger groups, Tregs and inflammatory markers increased in older groups (22). Aging is implicated in various pathways of ARDS pathogenesis, yet the precise mechanisms remain elusive. Therefore, further research is needed to understand the relationship between cellular aging, immune infiltration landscape, and their interplay in the context of ARDS disease.

Over the past decade, high-throughput sequencing has experienced rapid development and has permeated various fields of life sciences, significantly advancing the progress of basic medical research (23). GSE163426 is a dataset related to ARDS, containing a large number of samples (47 ARDS patients and five control individuals). In this study, we used various bioinformatics methods to obtain age-related characteristic genes for ARDS. Four hub ARDS-ARDEG genes demonstrated significant diagnostic performance and were validated in external datasets. Additionally, we corroborated the expression levels of the selected genes through animal experiments. Thymidylate Synthetase (TYMS) was identified as a promising diagnostic biomarker for ARDS in aging individuals. We assessed the enriched signaling pathways associated with TYMS expression and involvement in immune cell infiltration. Single-nucleus RNA sequencing highlighted elevated TYMS expression in endothelial cells, indicating its potential role in endothelial dysfunction seen in ARDS. These findings highlight TYMS's multifaceted involvement, particularly its modulation of immune responses and contribution to endothelial proliferation and vascular injury repair, presenting TYMS as a potential therapeutic target for precise intervention in ARDS among the elderly ICU population.

## 2 Materials and methods

### 2.1 Data sources

In our study, we acquired two bulk RNA sequencing (bulk-RNAseq) datasets, specifically GSE163426 and GSE84439, from the GEO database. The GSE163426 dataset was utilized as the training

set, encompassing 47 ARDS patients and five control individuals. The validation group, comprising seven sepsis patients and 8 ARDS patients, was derived from the GSE84439 dataset. Additionally, we utilized publicly available single-nucleus RNA sequencing (snRNA-Seq) data obtained from autopsy lung tissues of 19 COVID-19 patients and seven healthy donors. These data, including the corresponding clinical information, can be accessed at the GEO database using the accession number GSE171524.

## 2.2 Downloading and organizing aging-related genes

In order to identify ARGs for our study, we downloaded data from the HAGR database (<https://genomics.senescence.info/>) (24). This database comprises the GenAge dataset (307 genes) and the CellAge dataset (949 genes). After combining these datasets and eliminating duplicate genes, we obtained 1256 ARGs for subsequent analysis.

## 2.3 Identification of aging-related DEGs

To identify ARDEGs, we utilized the R package limma for differential analysis (25). The filtering criteria were set as  $|\log_{2}FC| > 1$  and  $P < 0.05$ . This analysis was performed on the ARDS and control samples. The intersection of the DEGs with the ARGs resulted in the identification of ARDEGs.

## 2.4 Construction of PPI network

Using the Search Tool for the Retrieval of Interacting Genes (STRING) database, we constructed a protein-protein interaction (PPI) network for evaluating the gene interactions among ARDEGs (26).

## 2.5 Functional and pathway enrichment analysis

The Kyoto Encyclopedia of Genes and Genomes (KEGG) and Gene Ontology (GO) were used in the functional enrichment analysis of ARDEGs (27). The GO analysis involved exploring the biological processes (BP), cellular components (CC), and molecular functions (MF) associated with these ARDEGs.

## 2.6 Weighted gene co-expression network analysis

The WGCNA analysis was conducted to construct a co-expression network in the GSE163426 dataset, utilizing the scale-free topology criterion (28). The dynamic tree-cutting method with a minimum module size of 30 was used to identify co-expressed gene modules. Gene significance (GS) values and module

membership (MM) values were employed to assess the association between gene modules and both ARDS and aging, ultimately determining the key modules.

## 2.7 Identification of hub ARDS-ARDEGs

The least absolute shrinkage and selection operator (LASSO), Random Forest (RF), and Extreme Gradient Boosting (XGBoost) algorithms were employed as the methods for screening and identifying key ARDS-ARDEGs. LASSO analysis was performed with the glmnet program, and 10-fold cross-validation was used to assess the penalty parameter (29). This approach outperforms traditional regression analysis methods in the assessment of high-dimensional data. XGBoost, a machine learning algorithm based on gradient boosting trees, was employed to assess the importance of ARDEGs in both ARDS and aging (30). The R package XGBoost aided in determining the significance of models constructed with various sets of ARDEGs. The random forest algorithm with recursive feature elimination (RFE) is a supervised machine learning method (31). The RFE approach was conducted by setting the number of decision trees to 500 and identifying aging-associated signature genes with relative importance greater than one. The intersection of aging-associated signature genes obtained through three machine learning filters using the R package Venn was defined as hub ARDS-ARDEGs. To assess the diagnostic utility of hub ARDS-ARDEGs in aging ARDS patients, the receiver operating characteristic curve (ROC) analysis was performed on the GSE1919 and GSE89408 datasets.

## 2.8 Experimental animals

This study was conducted in accordance with ethical guidelines and received ethical approval from the Ethics Committee of Hangzhou Hibio Technology Co., Ltd. (HB2311003). C57BL/6 mice, including males and females, were procured from Jiangsu Jiangsu Huachuang sino Pharma Tech Co., Ltd. The study utilized young mice (3 months old) and aged mice (18 months old). The ARDS mouse model was induced by intraperitoneal injection of lipopolysaccharide (LPS) (Sigma-Aldrich) at 5mg/kg for young mice and 2.5mg/kg for aged mice. Following 72 hours of LPS administration, the mice were euthanized, and lung tissues were collected for subsequent analysis.

## 2.9 Histopathological observation of lung tissue

Lung tissue was collected from the middle lobe of the right lung in mice. Following alcohol dehydration, paraffin embedding, and sectioning, the samples were stained with H&E and subsequently examined under an optical microscope to evaluate the extent of lung tissue damage. The freshly removed lung tissue from the left lobe was weighed using an analytical scale to obtain the wet weight (W). The tissue was then dried in an oven until a consistent weight was

reached to calculate the dry weight (D). To determine the degree of pulmonary edema, the formula  $W/D \times 100\%$  was applied to obtain the wet-to-dry weight ratio.

## 2.10 Quantitative real-time PCR

Reverse transcription of total RNA into complementary DNA (cDNA) was performed using the TOROBlue<sup>®</sup> qPCR RT Kit after RNA extraction from the upper lobe of the right lung was performed using Trizol (Vazyme). TOROGreen<sup>®</sup> qPCR Master Mix was used for qRT-PCR. The primer sequences for hub ARDS-ARDEGs are presented in Table S9 of the Supplementary Materials. Internal reference gene GAPDH was employed. Each group included six biological samples.

## 2.11 Analysis of SnRNA-seq data

The raw matrix in each dataset was normalized using the “LogNormalize” function in Seurat (version 4.3.1) (32). The “RunHarmony” function in the “harmony” package was utilized to reduce the batch effect (33). The “FindVariableFeatures” function was employed to select the top 2000 most variable genes as input data. Principal component analysis was used to determine the 19 best principal components for data integration. Following the acquisition of principal components, several cell types were distinguished using established cell-specific markers, and uniform manifold approximation and projection were utilized to view the cells.

## 2.12 Cell–cell communication analysis

Based on ligand-receptor interactions, cell-cell communication between several cell clusters was inferred and visualized using the R software’s “CellChat” package (34). The “CellChat” tool was used to import the snRNA-seq data that had been normalized using the “Seurat” package. We focused on the secreted signaling pathways and analyzed the communication between all cell types. Moreover, endothelial cells acted as signal senders and receivers in our particular analysis and visualization of the communication between these cells and other cell types.

## 2.13 Statistical analysis

R software (version 4.3.1) was used to conduct statistical analysis. Two groups were compared using Wilcoxon tests. The association between immune cell infiltration and hub ARDS-ARDEGs expression levels was examined using Spearman correlation analysis. A statistical significance threshold of  $P < 0.05$  was applied. The mean  $\pm$  standard deviation of a minimum of six independent experiments was used to present the statistical analysis of the qRT-PCR data, and unpaired two-tailed Student’s t-tests were employed to evaluate differences ( $*P < 0.05$ ;  $**P < 0.01$ ;  $***P <$

$0.001$ ). For statistical significance, a  $P$ -value of less than 0.05 was used.

# 3 Results

## 3.1 Identification of ARDEGs

The study’s procedural diagram is depicted in Figure 1. A total of 2448 DEGs between control and ARDS tracheal aspirates were identified, with 1312 genes up-regulated and 1136 genes down-regulated (Figure 2A). 134 ARDEGs were obtained by the intersection of ARGs and DEGs (Figure 2B; Supplementary Table S1). Using the R program limma, expression matrices of ARGs were taken out of the training set, and their differences were examined. A gene expression heat map was created to see the top 50 genes with the most significant differences (Figure 2C). A close association between ARDEGs at the protein level was found by the PPI protein network analysis (Figure 2D; Supplementary Table S2).

## 3.2 Functional enrichment analysis of ARDEGs

To understand the potential mechanisms of ARDEGs in ARDS and aging, we employed the R package clusterProfiler to perform GO and KEGG enrichment studies on ARDEGs (Supplementary Tables S3, 4). The GO enrichment analysis in BP showed that the first five ARDEG enrichments were primarily associated with protein phosphorylation, cellular response to DNA damage stimulus, negative regulation of apoptotic process, peptidyl-threonine phosphorylation, and positive regulation of transcription from RNA polymerase II promoter (Figure 3A). The top 20 enriched elements in MF and CC are shown in Figures 3B, C. Furthermore, these ARDEGs were considerably enriched in Cellular senescence, Cell cycle, FoxO signaling pathway, Longevity regulating pathway, and Autophagy (Figure 3D).

## 3.3 Construction of the weighted gene co-expression network

The R package WGCNA was employed for co-expression network construction, utilizing the variance in gene expression of the initial 75% of genes as a screening criterion. A total of 13,906 genes were encompassed in this network assembly. The determination of the soft threshold power at 12 yielded a scale-free index of 0.85, along with notably favorable mean connectivity, enabling the establishment of a scale-free network (Figures 4A, B). Following this, cluster analysis was conducted to identify highly analogous modules, resulting in the display of the cluster dendrogram (Figure 4C). The correlation among these modules was calculated (Figure 4D). The findings revealed a notable correlation between the MEmagenta module and ARDS ( $\text{cor}=0.34$ ;  $p=0.01$ ), as well as aging ( $\text{co}=-0.34$ ;  $p=0.01$ ) (Figure 4E; Supplementary Table S5). Moreover, a significant correlation

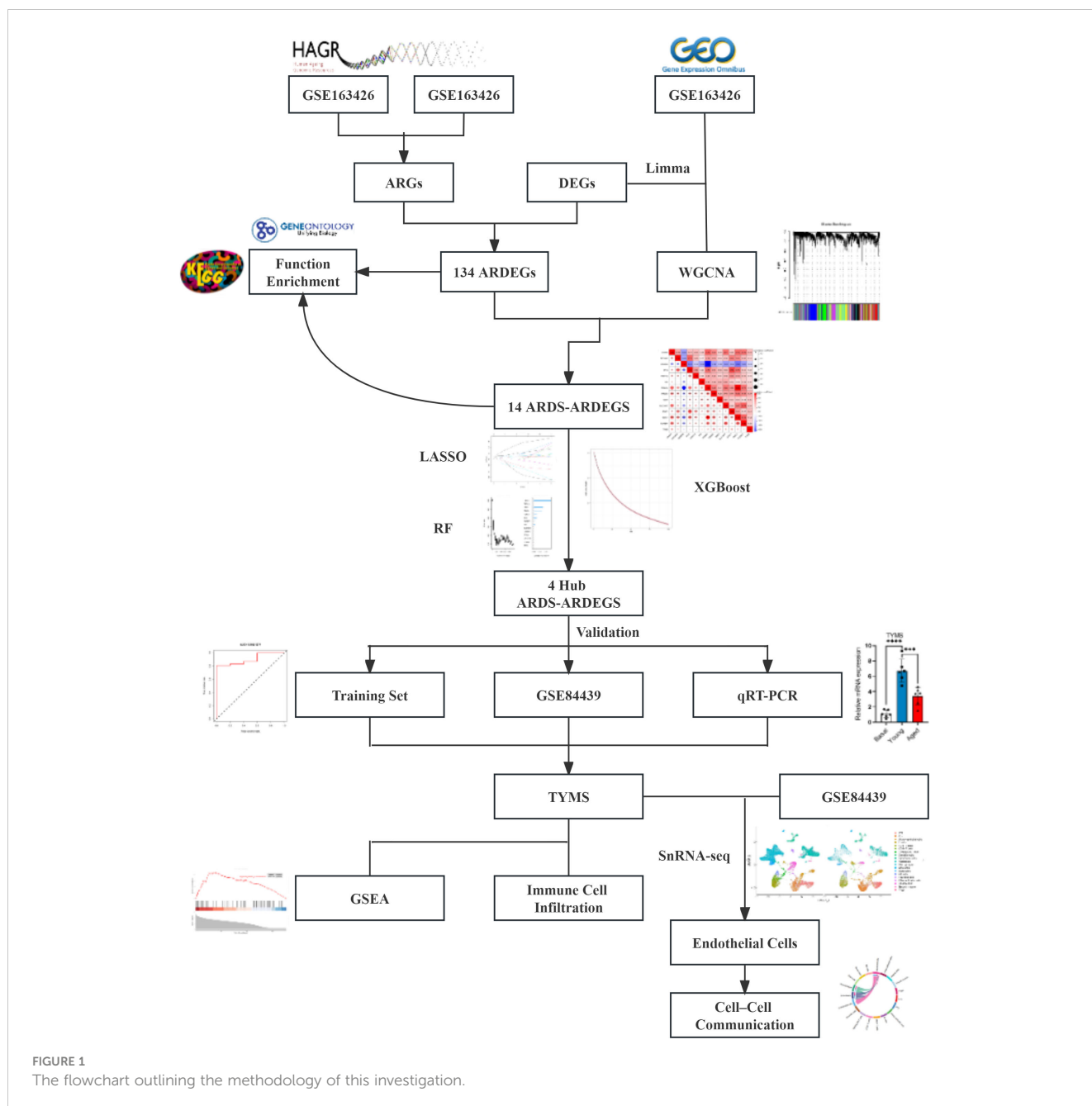


FIGURE 1  
The flowchart outlining the methodology of this investigation.

between MM and GS for ARDS within the magenta module ( $\text{cor}=0.3$ ;  $p=3.8\text{e-}14$ ) was observed, as well as aging ( $\text{co}=0.39$ ;  $p=1.4\text{e-}23$ ) (Figures 4F, G). The genes in the magenta module were selected as the candidate genes and compared with ARDEGs, resulting in the identification of 14 genes that were both in the magenta module and associated with ARDS and aging (Figure 4H).

### 3.4 Correlation and enrichment analysis of ARDS-ARDEGs

We used the Pearson correlation coefficient to assess the relationship between the ARDS-ARDEGs. PSMA2 exhibited a

high correlation with TTBPL1 ( $\text{cor}=0.84$ ) (Figure 5A). The KEGG pathway enrichment analysis demonstrated that the top ten enriched pathways associated with ARDS-ARDEGs were primarily involved in Spinocerebellar ataxia, Proteasome, Measles, Hepatitis C, Necroptosis, Influenza A, and the NOD-like receptor signaling pathway (Figure 5B; Supplementary Table S6). According to the GO enrichment analysis, ARDS-ARDEGs are enriched in BP, including the regulation of hematopoietic stem cell differentiation, deoxyribose phosphate biosynthetic process, negative regulation of G2/M transition of the mitotic cell cycle, regulation of the innate immune response, and deoxyribonucleotide biosynthetic process (Figures 5C, D; Supplementary Table S7). The map illustrating the interactions among BP was subsequently constructed (Figure 5E).

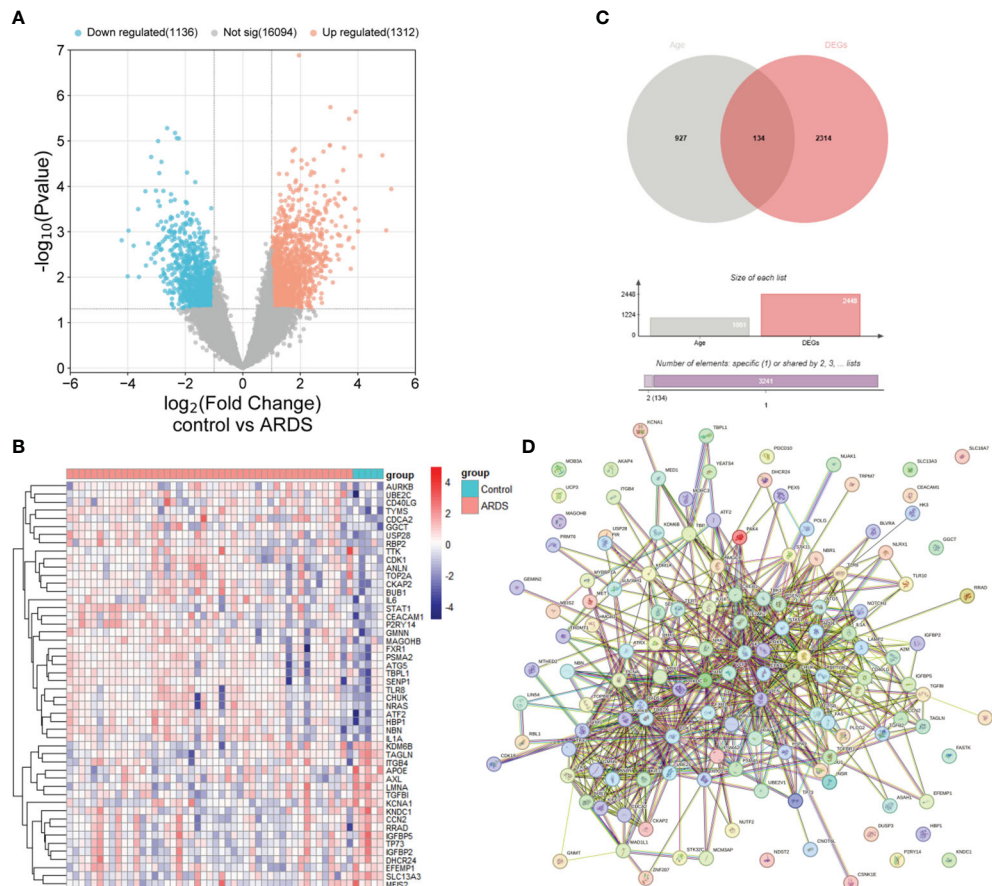


FIGURE 2

Identification of ARDEGs between control and ARDS. (A) The differential gene expression between the control and ARDS groups is displayed using a volcano plot. (B) A Venn diagram illustrates the overlap between ARGs and DEGs in the ARDS and control groups. (C) A heatmap is presented illustrating the expression patterns of the 50 most significant ARDEGs, based on the smallest p-values, in both the control and ARDS groups. (D) An interaction network map shows protein interactions among the 134 ARDEGs.

### 3.5 Identification of hub ARDS-ARDEGs via machine learning

Three machine learning algorithms were used to screen hub ARDS-ARDEGs in order to identify signature genes in the elderly population with ARDS: LASSO (Figures 6A, B), RF (Figures 6C, D), and XGBoost (Figure 6E). Following the integration of the outcomes from the three algorithms, we ultimately identified four hub genes: CKAP2, P2RY14, RBP2, and TYMS (Figure 6F; Supplementary Table S8).

### 3.6 Diagnostic efficacy of hub ARDS-ARDEGs

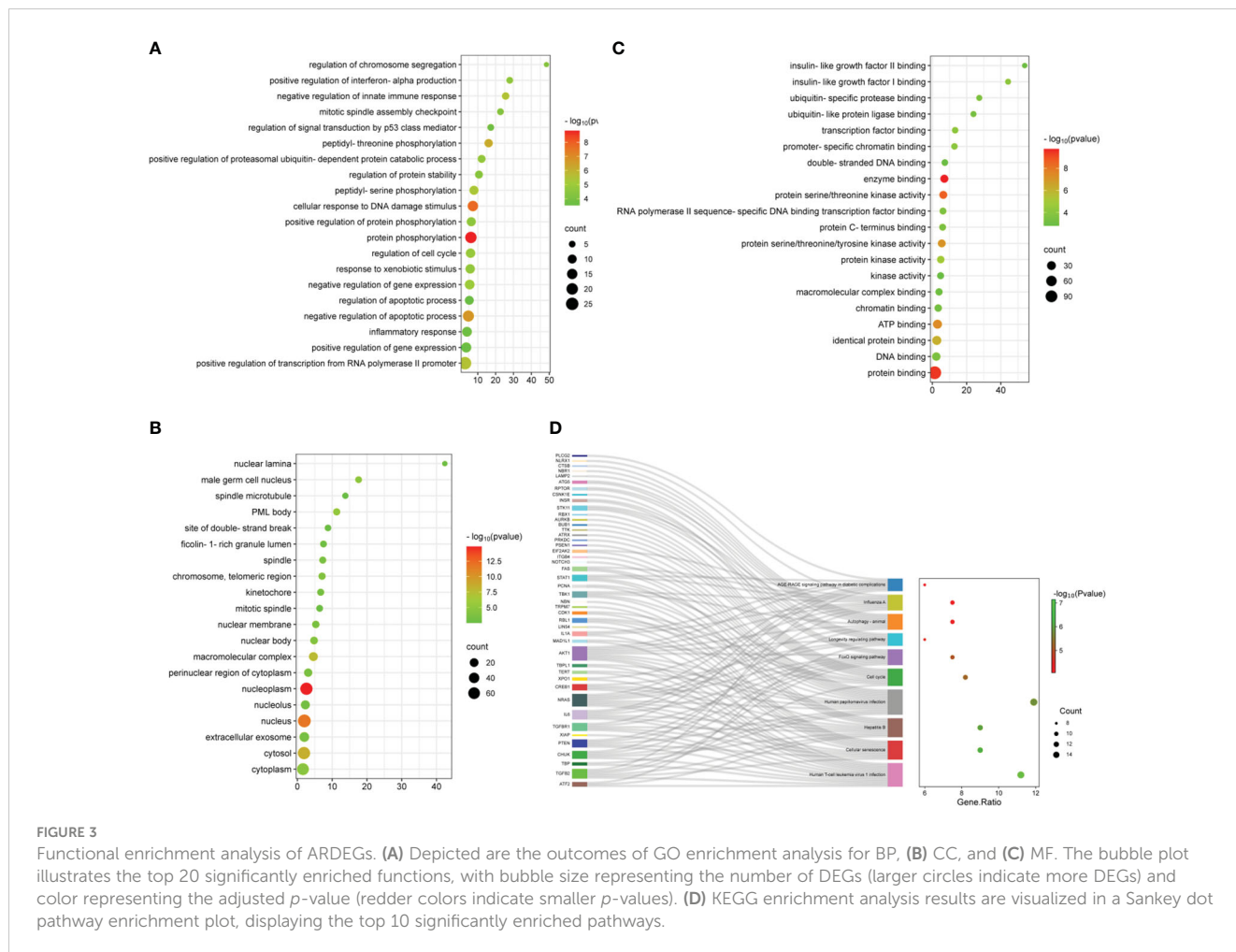
The ROC analysis revealed that the four hubs ARDS-ARDEG had high diagnostic values in the training set. The area under the curve (AUC) of ROC for these signature genes was observed as follows: 0.902 for CKAP2, 0.843 for P2RY14, 0.770 for RBP2, and 0.834 for TYMS (Figures 7A–D). Furthermore, the screened signature genes demonstrated higher expression levels in individuals with ARDS than those in the healthy control group, indicating a potential role of

these genes in the pathogenesis of ARDS (Figures 7E–H). Subsequently, a correlation analysis was conducted between patient age and the expression of hub ARDS-ARDEGs (Figures 7I–L). As patient age increased, the expression of these genes decreased, with TYMS demonstrating the strongest correlation with the aging process.

In addition, the diagnostic efficacy of each signature gene in predicting ARDS was evaluated in an external validation cohort. By GSE84439, the AUC values of ROC for CKAP2, P2RY14, RBP2, and TYMS were 0.411, 0.321, 0.607, and 0.821, respectively (Figures 8A–D). In comparison to sepsis patients, only TYMS demonstrated significant changes in expression among these characteristic genes in ARDS patients, indicating a remarkable upregulation (Figures 8E–H). These observations indicate that TYMS exhibits superior diagnostic efficiency for ARDS, irrespective of whether it is used to distinguish elderly ARDS patients or differentiate sepsis patients.

### 3.7 Aging inhibited TYMS induction in mice after ARDS modeling

The murine model of ARDS was established by administering LPS to both aged (18 months) and young (3 months) mice. Despite



being challenged with a lower dose of LPS (2.5 mg/kg) compared to young adult mice (5 mg/kg), aged mice exhibited more severe lung injury (Figures 9A, B). At 72 hours after LPS administration, aged mice exhibited lung edema, a condition not observed in young adult mice (Figure 9C). To confirm the mRNA expression levels of hub ARDS-ARDEGs, qRT-PCR was performed on total mRNA extracted from lung tissues (Figures 9D–G). After ARDS modeling, the expression of characteristic genes CKAP2, P2RY14, RBP2, and TYMS was significantly altered. Notably, there was a significant disparity in TYMS expression between the young and aged mice after modeling. The findings demonstrated that the four characteristic genes were strongly activated following the onset of ARDS, whereas aging inhibited the proper induction of TYMS expression in the progression of ARDS.

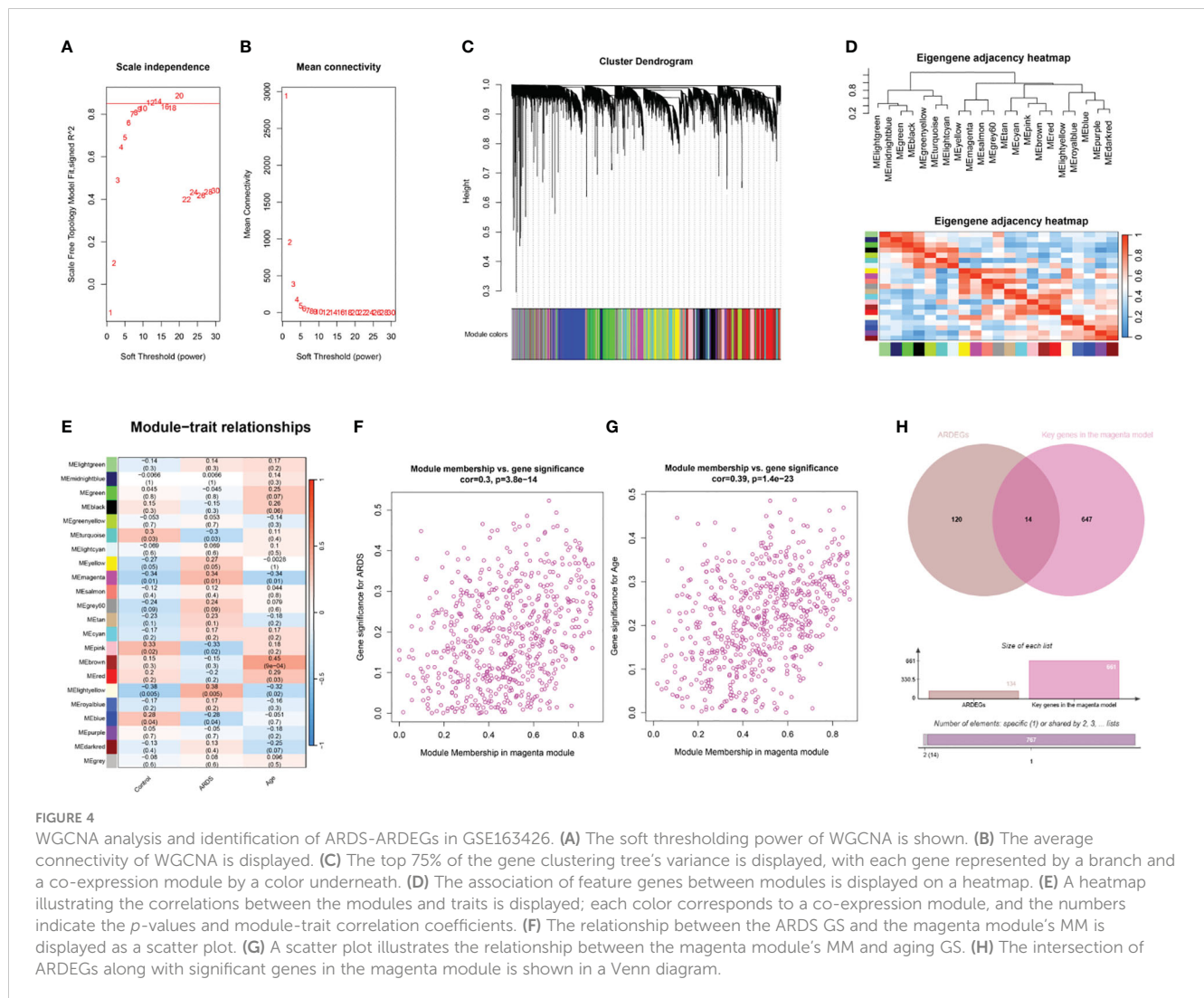
### 3.8 Difference analysis and GSEA analysis of TYMS grouping

Based on the median TYMS value and a significant threshold of “ $P < 0.05$ ” and “ $|\log_2FC| > 1$ ,” tracheal aspirate samples from ARDS patients in the GSE163426 dataset were classified into two groups: a high-expression group and a low-expression group. As a result, 582 genes exhibited up-regulation, and 544 genes displayed down-regulation

(Figure 10A). The heat map depicted the top 30 DEGs (Figure 10B). To evaluate the signaling pathways linked to TYMS, GSEA analysis was conducted (Figures 10C–H). The findings demonstrated a significant correlation between TYMS and the regulation of immune system processes, defense response, negative regulation of alpha-beta T cell activation, blood vessel morphogenesis, regulation of cell population proliferation, and negative regulation of inflammatory response.

### 3.9 Evaluation and analysis of immune cell infiltration

The single-sample gene set enrichment analysis (ssGSEA) algorithm was employed to analyze immune cell infiltration, aiming to discern immunological features (Supplementary Table S10). In ARDS samples, the infiltration levels of Activated CD4 T cells, Activated CD8 T cells, and Effector memory CD4 T cells were significantly increased compared to the healthy control. Conversely, the infiltration of CD56<sup>dim</sup> natural killer cells and Natural killer cells in ARDS samples was significantly reduced (Figure 11A). Following this, a correlation analysis was conducted, linking the expression of hub genes with immune cell infiltration in ARDS patients (Figure 11B). Notably, a strong correlation exists between TYMS expression and the infiltration of various immune cells. Subsequent



analysis involved grouping individuals based on TYMS expression levels to explore the relationship between TYMS and immune cell proportion (Figure 11C). The analysis revealed a significant upregulation in the proportion of activated B cells, Memory B cells, and Type 2 T helper cells in the group exhibiting high TYMS expression.

Conversely, there was a distinct decrease in the proportion of CD56<sup>dim</sup> natural killer cells, Central memory CD4 T cells, and Immature dendritic cells. Figures 11D–I demonstrate the six correlations between TYMS and the immune cells. These findings indicate an association between TYMS and the regulation of immune responses, thereby enhancing the ability to resist pathogenic microorganisms and inhibiting excessive inflammatory responses.

### 3.10 Discrimination of cell source of TYMS at single-cell resolution

To investigate the cellular origin of TYMS, we acquired snRNA-Seq data, including data from autopsy lung tissues of approximately 116,000 nuclei taken from the lungs of nineteen individuals who

died from COVID-19 and seven control individuals from GSE171524. Based on the clinical information of these 19 patients, it is evident that they were over 55 and presented with concomitant respiratory symptoms. Unsupervised analysis identified 19 distinct cell clusters (Figure 12A). These clusters were recognized as distinct cell types based on the expression levels of established markers: alveolar type I (AT1) cells, alveolar type II (AT2) cells, airway epithelial cells, B cells, CD4<sup>+</sup> T cells, CD8<sup>+</sup> T cells, cycling NK/T cells, dendritic cells, endothelial cells, fibroblasts, macrophages, mast cells, monocytes, NK cells, neuronal cells, other epithelial cells, plasma cells, smooth muscle cells, and Tregs. The disruption of alveolar epithelial and endothelial barriers was attributed to the loss of AT1 cells, AT2 cells, and endothelial cells and the proliferation of mononuclear/macrophage cells, fibroblast cells, and neuronal cells (Figure 12B). It was discovered that endothelial cells exhibited high TYMS expression (Figure 12C). Compared to the control group, patients with respiratory symptoms manifested a discernible upregulation in TYMS expression within endothelial cells (Figure 12D). The findings above indicate that TYMS is primarily expressed in endothelial cells, and moderate induction may contribute to endothelial regeneration and the

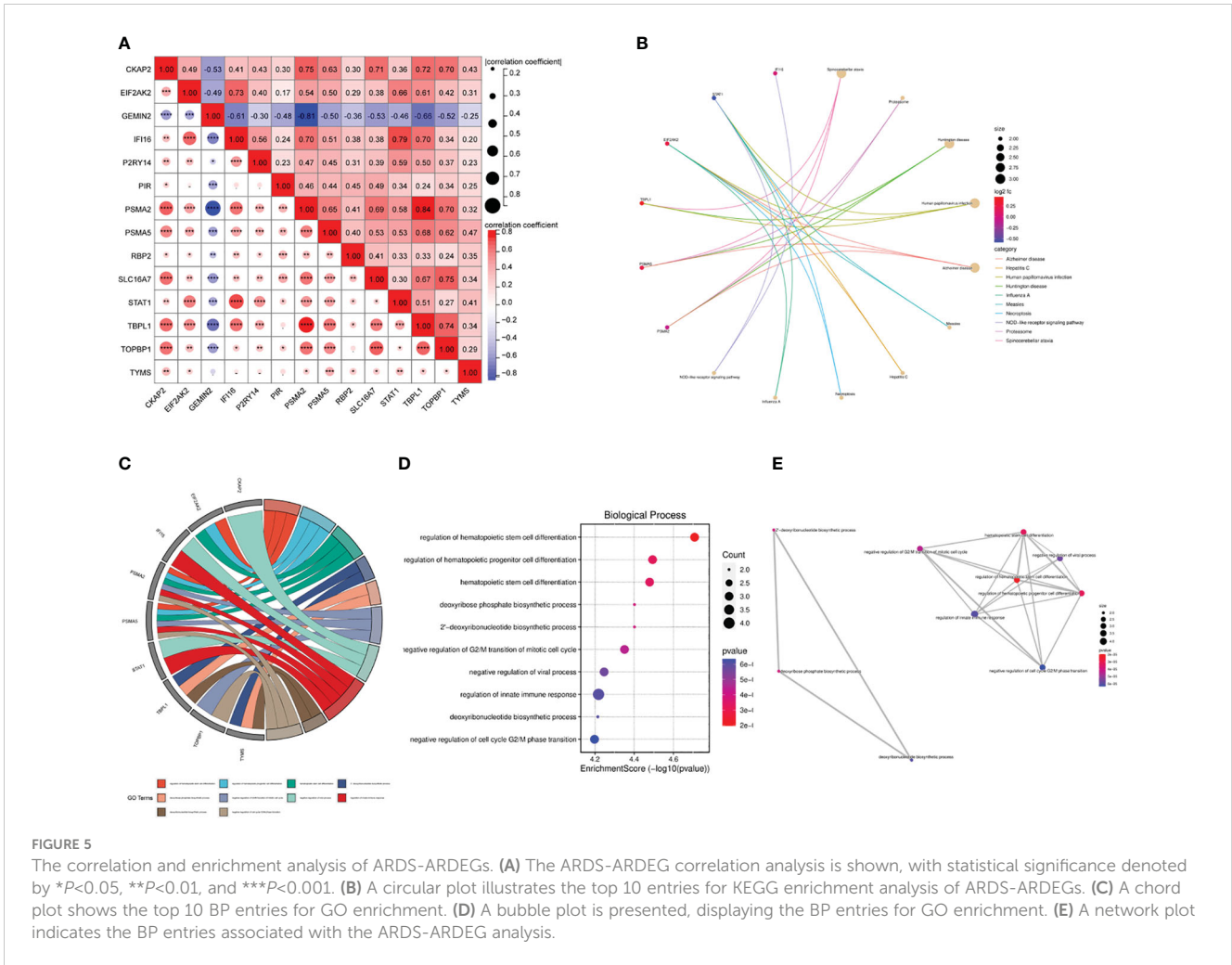


FIGURE 5

The correlation and enrichment analysis of ARDS-ARDEGs. (A) The ARDS-ARDEG correlation analysis is shown, with statistical significance denoted by \* $P < 0.05$ , \*\* $P < 0.01$ , and \*\*\* $P < 0.001$ . (B) A circular plot illustrates the top 10 entries for KEGG enrichment analysis of ARDS-ARDEGs. (C) A chord plot shows the top 10 BP entries for GO enrichment. (D) A bubble plot is presented, displaying the BP entries for GO enrichment. (E) A network plot indicates the BP entries associated with the ARDS-ARDEG analysis.

maintenance of endothelial barrier integrity, thereby reducing the infiltration of inflammatory cells and inhibiting the progression of ARDS.

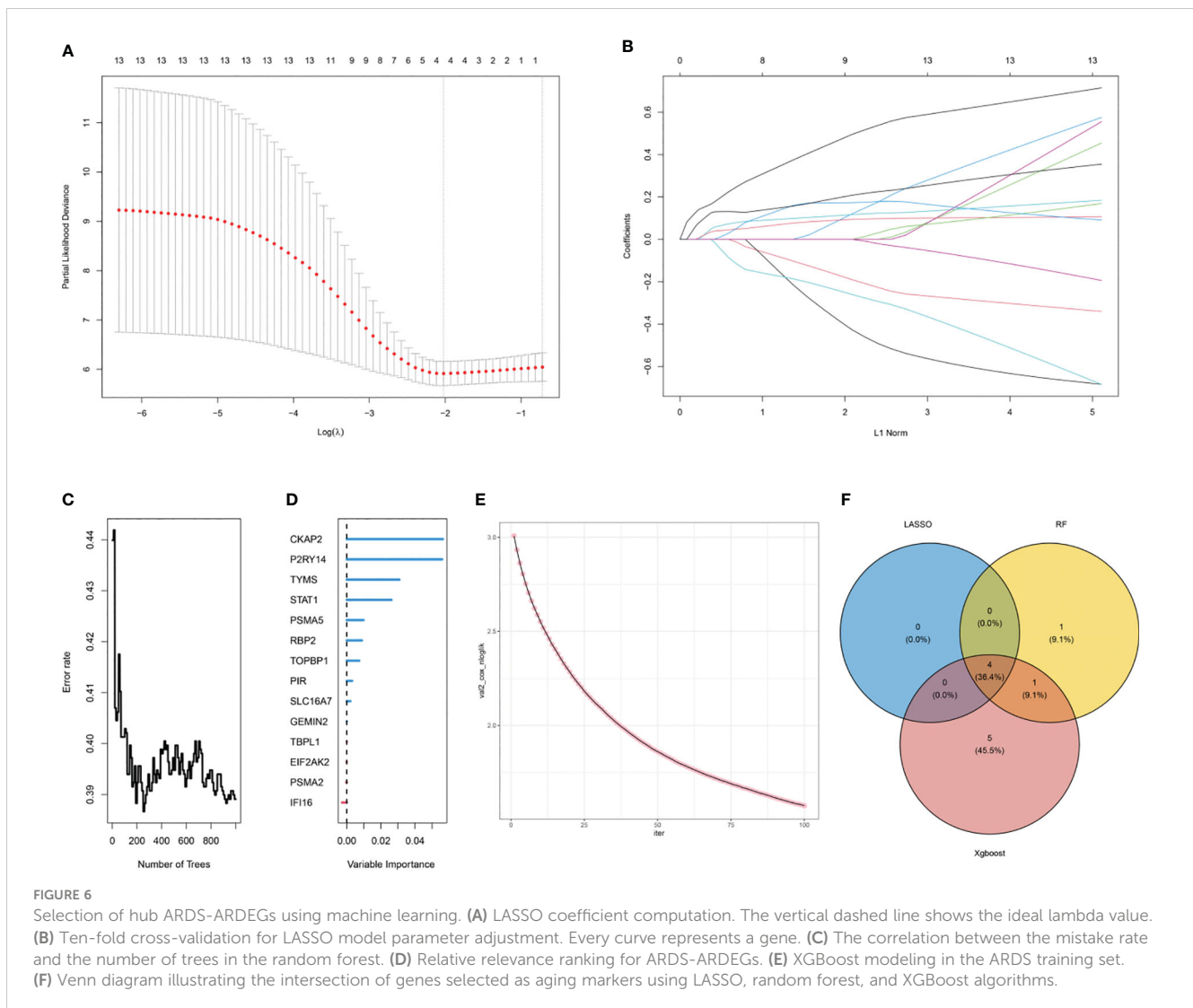
### 3.11 Investigation of communication between endothelial cells and other cell types

In order to evaluate intercellular communication, expression levels of ligands and their matching receptors are examined. The results above indicate that TYMS is primarily expressed in endothelial cells and is associated with immune cell infiltration. To investigate intercellular communication further, we employed the “CellChat” software package for a comprehensive analysis. Circular plots were generated to visualize the secretion signals involved in intercellular communication across all cell types (Figures 13A, B). The analysis demonstrated that endothelial cells communicate with airway epithelial cells through the VISFATIN signaling pathways (Figure 13C). Moreover, endothelial cells primarily receive signals from AT1 cells, fibroblasts, smooth muscle cells, neuronal cells, fibroblasts, and macrophages (Figure 13D).

Furthermore, we conducted a ligand-receptor pair analysis that identified specific signaling interactions. Endothelial cells were found to preferentially send signals via the NAMPT - INSR pathway while receiving signals through the VEGFA - VEGFR1, IGF1 - IGF1R, ANGPT1 - TEK, SEMA3A - (NRP1+PLXNA2), SEMA3C - (NRP1+PLXNA2), and SEMA3D - (NRP1+PLXNA2) pathways (Figures 13E, F). Intercellular communication between endothelial cells and other cells is predominantly mediated by the SEMA3 signaling pathway, with endothelial cells serving as the primary receiver cells in this pathway (Figure 13G). The SEMA3 signaling pathway exerts a significant influence on the vascular system, contributing to the development and regeneration of blood vessels. Conclusively, these discoveries provide invaluable perspectives on the intercellular dialogue between endothelial cells and various cell types, shedding light on the distinct signaling pathways and molecules implicated in this intricate process.

## 4 Discussion

ARDS is a common and severe respiratory condition, particularly in the elderly (35). Extensive research has established a close association between ARDS and the patient’s systemic or



localized inflammatory response, with impairment of the pulmonary endothelial barrier function significantly contributing to lung injury and poor prognosis in sepsis and ARDS (36). Accumulating evidence also emphasizes the role of aging in this context, as ARDS incidence and mortality rates are increased in the elderly population ( $\geq 65$  years old) (37). Research conducted by Soo Jung Cho et al. suggests that the susceptibility of the elderly to pulmonary diseases may be related to age-related changes in the composition and functionality of endothelial cells (11). Relevant studies have found elevated levels of ATP2B1 expression in ARDS patients, which is associated with endothelial barrier disruption (38). Aging impairs lung resident endothelial cell-mediated endothelial regeneration, leading to persistent inflammatory lung injury and high mortality rates (39). Aging exposes the immune system to sustained immune stressors and inflammatory assaults, contributing to immune senescence (40). These findings provide a solid basis to support the potential link between aging and immune regulation in ARDS.

With the current application of bioinformatics in the field of medicine, new avenues have opened up for scientific research on

ARDS, allowing for the discovery of potential essential target genes. This study combines bioinformatics analysis with machine learning strategies to investigate the pathogenesis of ARDS from an aging perspective.

Through our analysis of normal and ARDS patient samples, we have identified 134 ARDEGs. Based on the results of GO and KEGG enrichment analyses, these ARDEGs are primarily involved in cellular responses to DNA damage stimuli, inflammatory reactions, negative regulation of innate immunity, and the FoxO signaling pathway and cellular senescence pathway. Our research highlights the involvement of these genes in inflammation response and aging. Increasing evidence supports the influence of aging on the occurrence of ARDS. For instance, elevated levels of reactive oxygen species production enzyme NADPH oxidase 4 in aging mice enhance endothelial cell permeability, impairing endothelial barrier function (41).

Additionally, KEGG pathway enrichment analysis indicates that these ARGs predominantly participate in the FoxO signaling pathway and lifespan regulation. FOXO transcription factors are crucial determinants of aging and longevity (42). Further research is needed to explore the hub ARDS-ARDEGs.

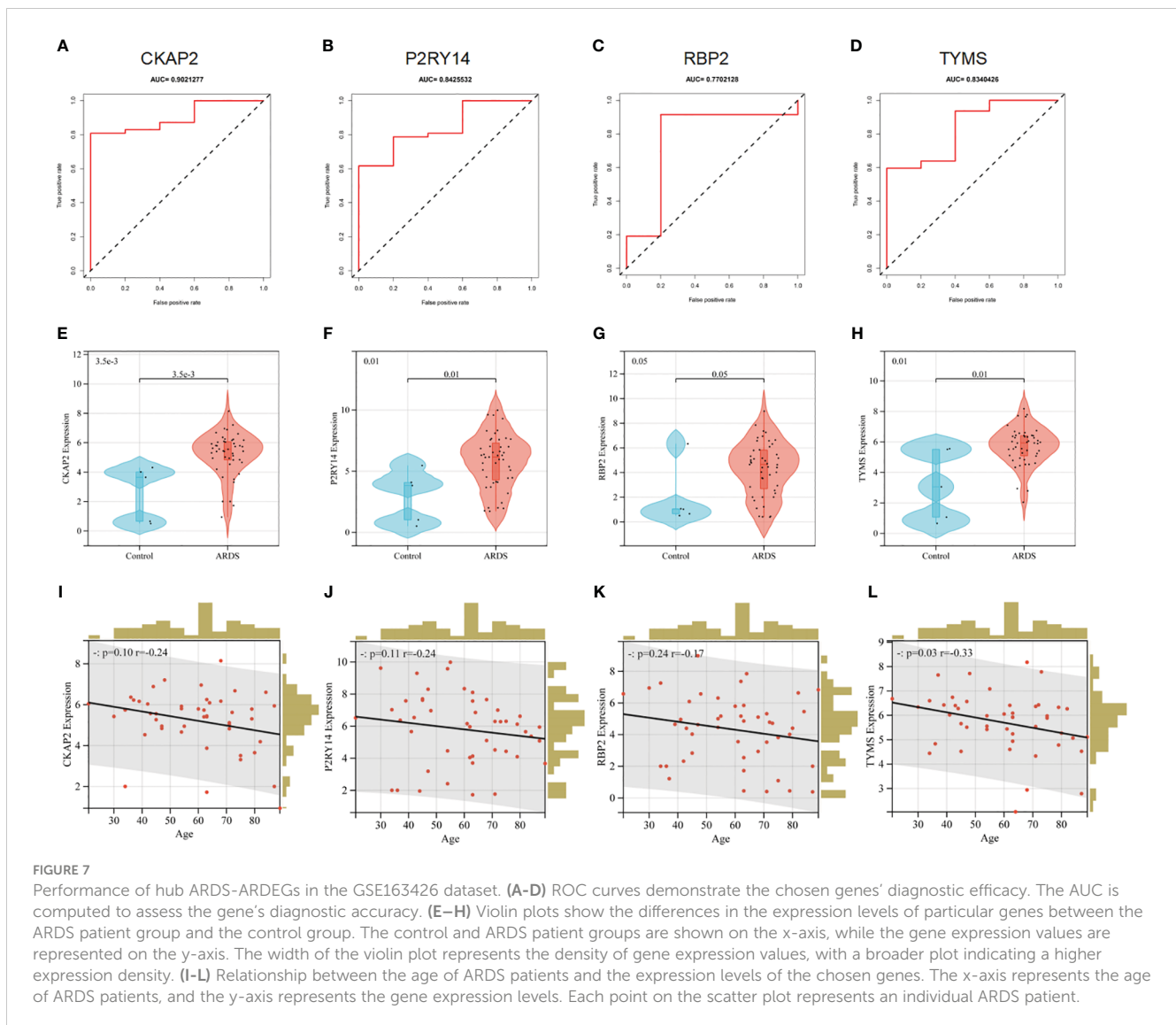


FIGURE 7

Performance of hub ARDS-ARDEGs in the GSE163426 dataset. (A–D) ROC curves demonstrate the chosen genes' diagnostic efficacy. The AUC is computed to assess the gene's diagnostic accuracy. (E–H) Violin plots show the differences in the expression levels of particular genes between the ARDS patient group and the control group. The control and ARDS patient groups are shown on the x-axis, while the gene expression values are represented on the y-axis. The width of the violin plot represents the density of gene expression values, with a broader plot indicating a higher expression density. (I–L) Relationship between the age of ARDS patients and the expression levels of the chosen genes. The x-axis represents the age of ARDS patients, and the y-axis represents the gene expression levels. Each point on the scatter plot represents an individual ARDS patient.

We identified four hub ARDS-ARDEGs (CKAP2, P2RY14, RBP2, and TYMS) using WGCNA analysis and three machine learning screenings (LASSO, RF, XGBoost). Our results indicated that four hub ARDS-ARDEGs were considerably elevated in samples from ARDS patients and had a robust diagnostic ability to predict ARDS.

CKAP2 (Cytoskeleton-associated protein 2, a crucial protein that controls cell proliferation), particularly during mitosis and cytokinesis (43). CKAP2 is up-regulated in a variety of malignant tumors and has diagnostic value in osteosarcoma (44), triple-negative breast cancer (45), gastric cancer, and other tumors (46). It has been reported that the CKAP2 gene plays a role in cell senescence (47), but its pathway needs to be confirmed by further studies. TYMS (Thymidylate synthase) is a gene that plays a crucial role in DNA replication and repair (48). Chen Y reported that the knockdown of TYMS resulted in reactive oxygen species generation, DNA damage, and cellular senescence (49). Restoring the expression and activity of FoxM1 may potentially enhance the functionality of endothelial cells and promote vascular neogenesis and repair (50). Additionally, as a downstream target of FoxM1,

TYMS could be involved in the endothelial cell repair process (51). RBP2 (Retinoblastoma binding protein 2) facilitates the uptake, absorption, and metabolism of retinol (52). Moreover, it is implicated in the development of obesity and associated metabolic disorders (53). Several studies indicate that RBP2 plays a central role in maintaining innate immunity in the intestinal tract (54). Nevertheless, extensive research is still required to attain a comprehensive understanding of RBP2's role in ARDS pathology. P2RY14, a G-protein coupled purinergic receptor, manifests its expression within the placenta, adipose tissue, intestine, stomach, and lung (55). Under conditions of tissue stress, alterations in the expression levels of P2Y14 occur, thereby influencing the processes of cellular aging and apoptosis (56). The expression of P2Y14R in human alveolar epithelial type 2 cells and its impact on IL-8 secretion and neutrophil recruitment suggest its pivotal role in the activation of airway epithelial cells and modulation of immune response (57).

To further validate the results of the bioinformatics analysis, we conducted qRT-PCR to identify and screen the four hub genes using

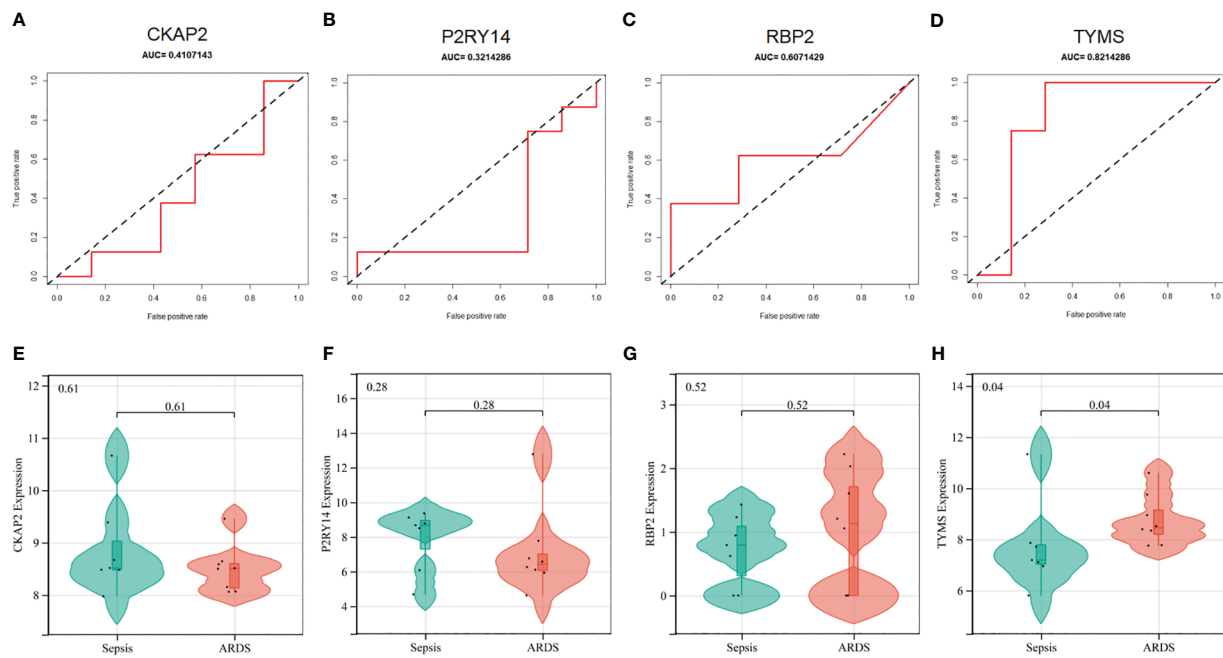


**FIGURE 8** Performance of hub ARDS-ARDEGs in the GSE84439 dataset. (A-D) Violin plots compare the expression levels of particular genes in patients with ARDS and those with septic shock. (E-H) ROC curves indicate the diagnostic performance of the identified genes about ARDS.

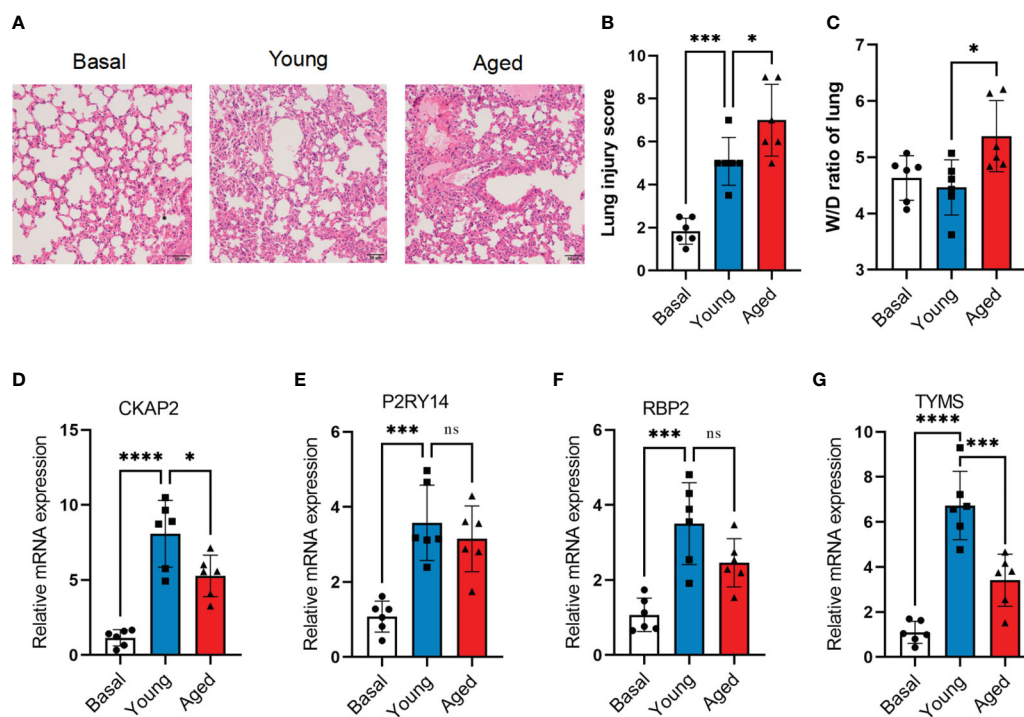


**FIGURE 9** Validation of hub ARDS-ARDEGs through total RNA sequencing. (A) Histopathological images of lung tissues in LPS-induced ARDS young and aged mice. Scale bar, 50  $\mu$ m. (B) Lung injury scoring analysis based on alveolar wall congestion and inflammatory cell infiltration, bronchovascular peribronchial hemorrhage and inflammatory cell infiltration, bronchial lumen exudate, and endothelial cell swelling, with assignment of each slide area to a severity score ranging from 1 (average) to 4 (severe injury). (C) Lung wet-to-dry ratio in young adult and aged mice 72 hours post LPS exposure. (D-G) CKAP2, P2RY14, RBP2, and TYMS expression levels in young and aged ARDS mouse models, n = 6 in each group. The data are shown as mean  $\pm$  standard deviation, and asterisks (\* $p$ <0.05, \*\* $p$ <0.01, \*\*\* $p$ <0.001, \*\*\*\* $p$ <0.0001) denote statistical significance; "ns" indicates no significance.

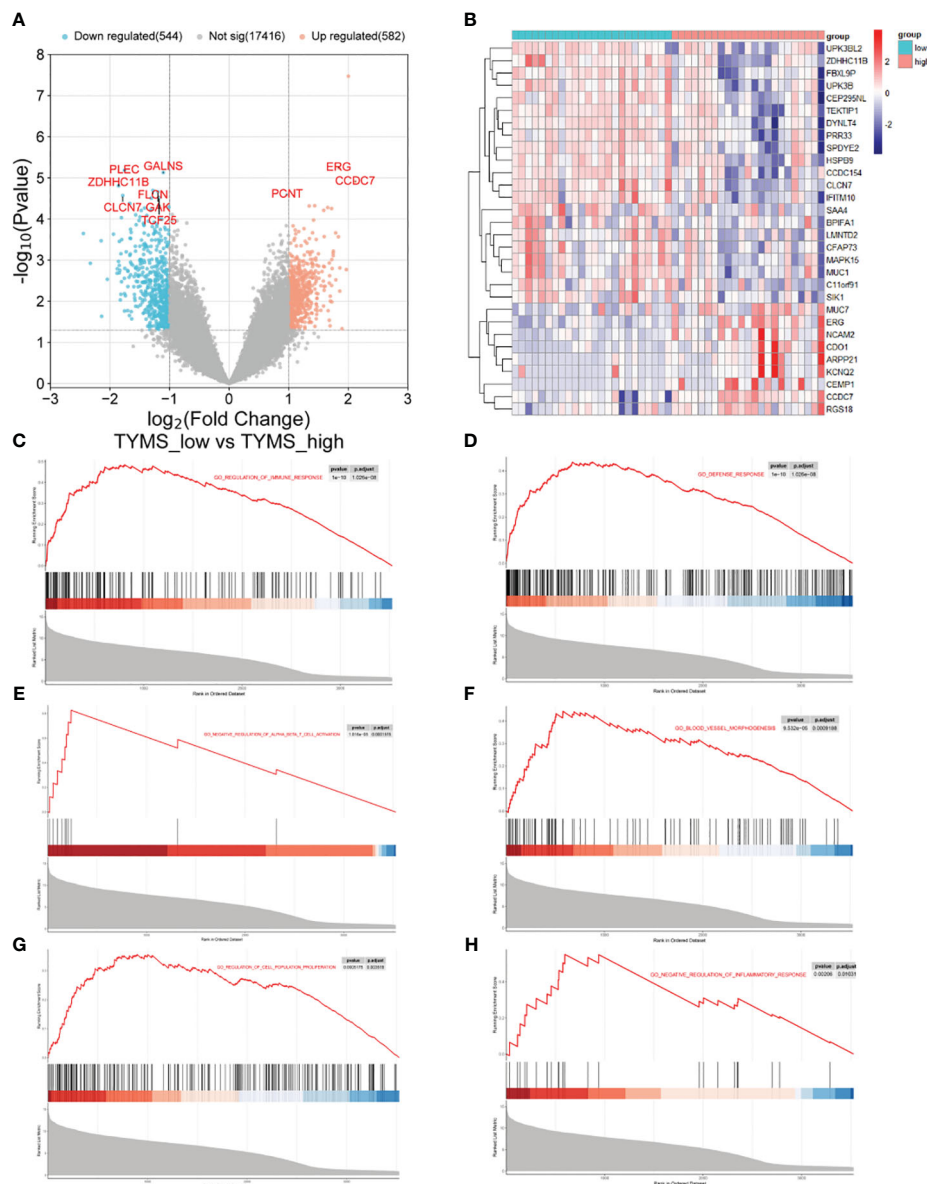


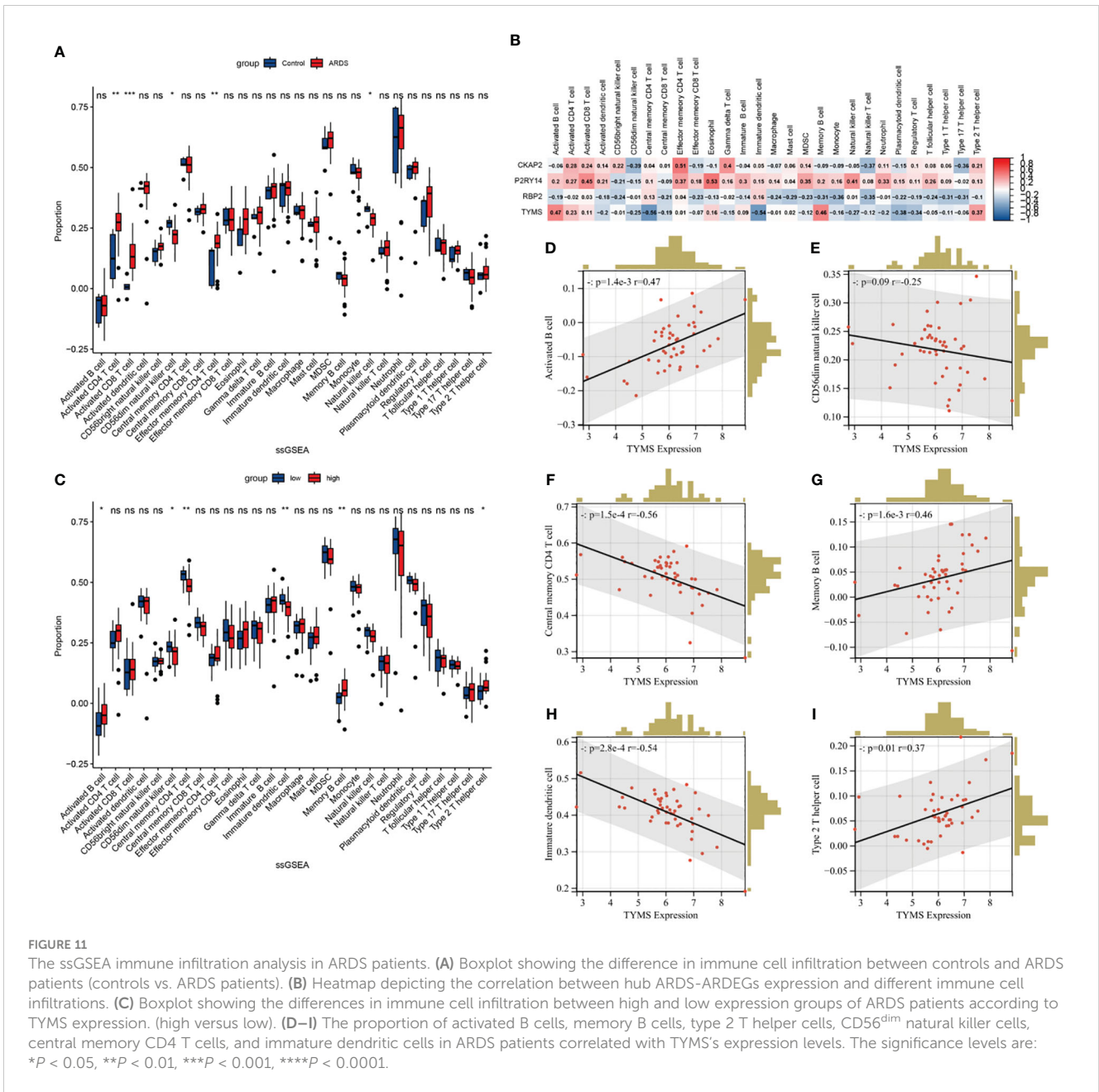
FIGURE 10

The GSEA of different TYMS expression groups in ARDS patients. (A) A volcano plot shows the differential gene analysis results between the ARDS patient groups with high and low TYMS expression. (B) A cluster heat map, ordered by  $p$ -value, displaying the top 30 genes linked to TYMS that are differentially expressed. (C–H) In the TYMS high expression group of ARDS patients, enrichment analysis reveals the upregulation of signaling pathways involved in the regulation of immune system processes, defense response, negative regulation of alpha-beta T cell activation, blood vessel morphogenesis, regulation of cell population proliferation, and negative regulation of inflammatory response in the TYMS high expression group of ARDS patients.

lung tissue samples from both the control and ARDS model groups of mice. Remarkably, we observed significantly higher expression levels of all four genes in the lung tissues of ARDS mice, aligning with the findings of the bioinformatics analysis. Notably, there was a significant difference in TYMS expression between elderly and young mice after modeling, suggesting its potential as a diagnostic biomarker for elderly ARDS patients. Therefore, our subsequent research will focus on TYMS as the target gene for further exploration.

To investigate the possible biological functions and pathways TYMS may be involved in ARDS, we divided the ARDS dataset

GSE163426 into groups based on the expression levels of TYMS and performed GSEA. The results revealed that TYMS plays a critical role in ARDS development by influencing immune inflammation and vascular morphogenesis. These findings are consistent with previous research on ARDS. We then conducted further research to evaluate the immunological infiltration in ARDS utilizing ssGSEA. In ARDS samples, we discovered a substantial increase in the infiltration levels of effector memory CD4 T cells, activated CD8 T cells and activated CD4 T cells. Additionally, TYMS demonstrated a negative correlation with CD56<sup>dim</sup> natural killer cells, Central memory CD4 T cells, and immature dendritic cells,

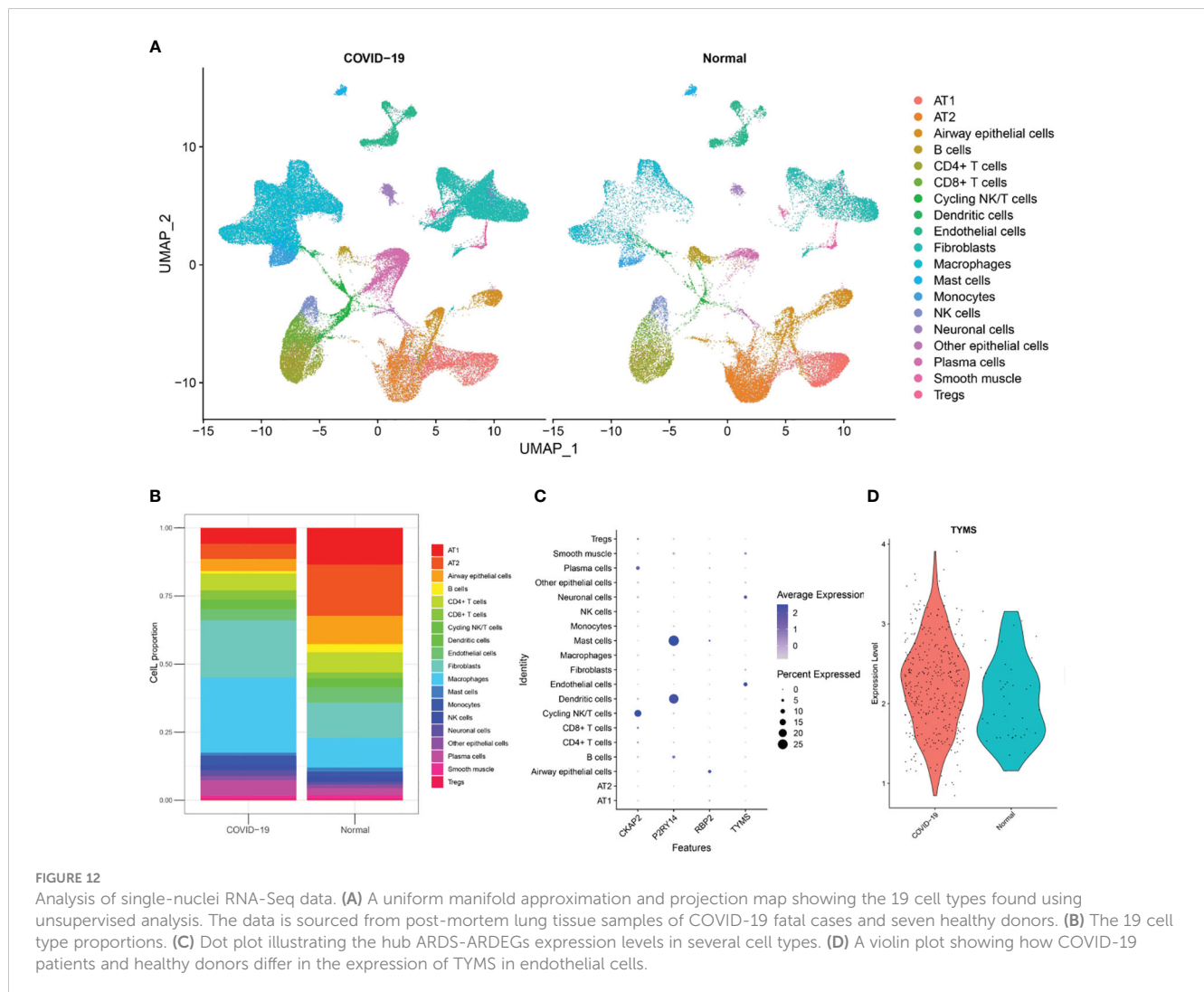


and a positive correlation with activated B cells, memory B cells, and Type 2 T helper cells by correlation analysis with immune cells. It has been established that inflammatory and immune-infiltrating cells, such as Type 2 T helper cells, which are mainly responsible for producing IL-4, IL-5, and IL-13 involved in humoral immunity, serve a purpose in the development of ARDS (58).

However, the intricate interaction among these immune cells, their distinct roles in ARDS, and the intricate molecular mechanisms involved still require further investigation for a comprehensive understanding.

Furthermore, we investigated the cellular localization of TYMS based on snRNA-Seq data. The results revealed different proportions of AT1 cells, AT2 cells, endothelial cells, mononuclear/macrophage

cells, fibroblast cells, and neuronal cells between the control group and COVID-19-ARDS patients. Remarkably, the proportion of endothelial cells in ARDS patients was significantly lower compared to the healthy control group, indicating impaired endothelial cell function in ARDS patients. The increased proliferation of B cells is associated with improved survival rates in ARDS (59). Additionally, there was a decrease in alveolar epithelial cells in ARDS patients, consistent with the findings of a study by Feng et al. (60). TYMS showed high expression in the endothelial cells of ARDS patients, and moderate induction may contribute to endothelial regeneration and the maintenance of endothelial barrier integrity, thereby reducing the infiltration of inflammatory cells and inhibiting the progression of ARDS.



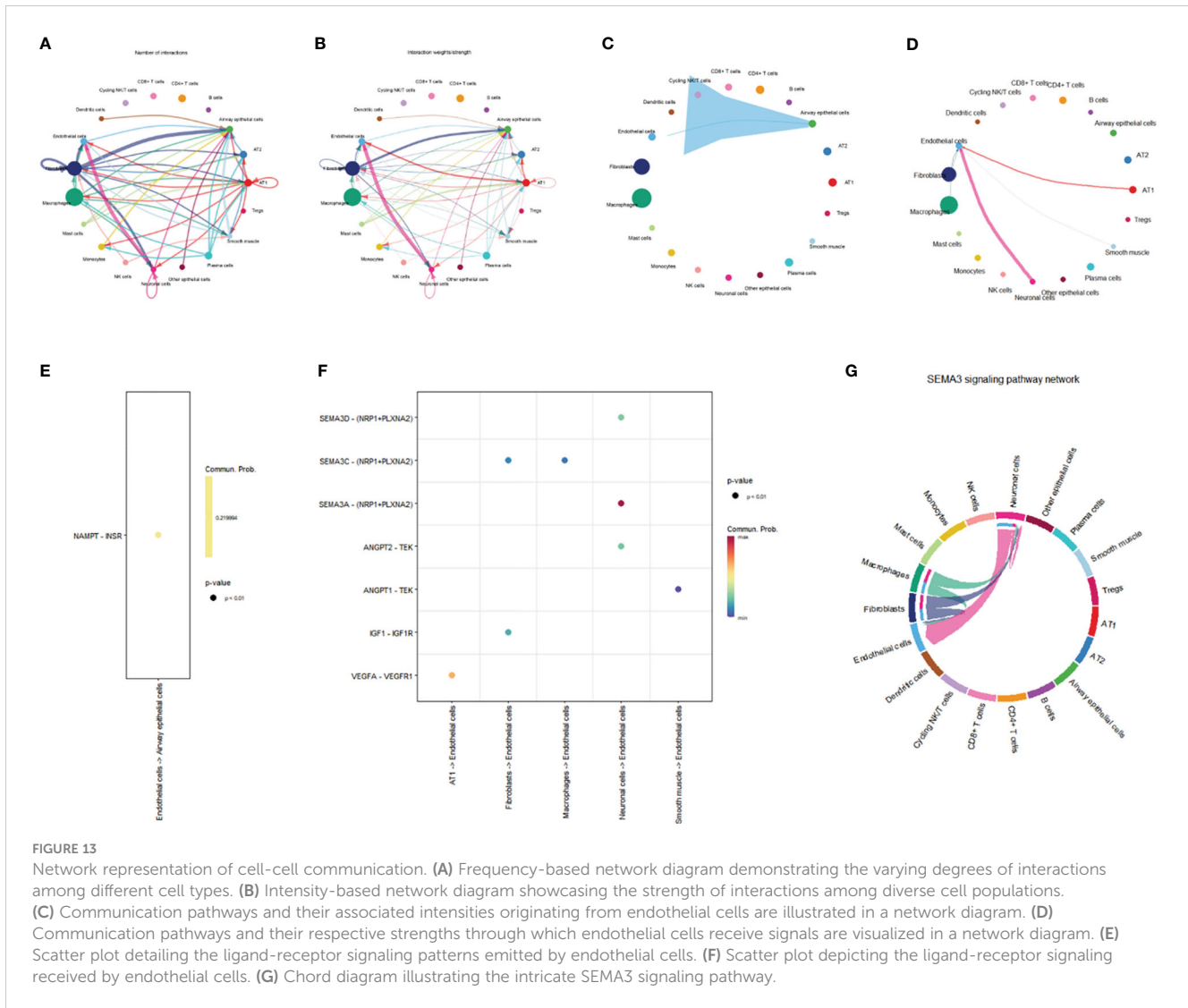
Within the microenvironment of the tissue, intercellular communication among diverse cell types assumes a consequential role. The results of this study demonstrate that endothelial cells communicate with airway epithelial cells through the VISFATIN signaling pathway. Additionally, endothelial cells receive ligand signals from other cell types, including AT1 cells, fibroblast cells, smooth muscle cells, neurons, fibroblast cells, and macrophages. The SEMA3 signaling pathway mainly mediates cell-to-cell communication between endothelial cells and other cells. The SEMA3 signaling pathway significantly impacts the vascular system, promoting vascular development and regeneration (61). In conclusion, these findings provide valuable insights into the intercellular communication between endothelial cells and other cell types, elucidating the specific signaling pathways and molecules involved.

Our research has limitations. Firstly, information from open databases served as the foundation for all analysis. The species representation, sequencing platforms, molecular types, sample grouping, and sample quality of the GEO collection are all limited. Nevertheless, the datasets utilized in this investigation were the only ones readily available for our analysis. Even though

our cohorts have been constructed and confirmed, prospective research with additional validation would be ideal. Extensive research is also required to investigate the possible roles of hub genes in the pathophysiology of ARDS.

## Conclusion

Our study utilized bioinformatics analyses and machine learning methods to identify four potential aging-related genes associated with ARDS. The essential genes CKAP2, P2RY14, RBP2, and TYMS were validated using animal samples to determine their expression levels in an animal model through the protective role of TYMS in maintaining the integrity of the pulmonary microvascular endothelial barrier, promoting endothelial cell regeneration, and restoring its function. It could be a novel approach to the management and prevention of ARDS. These discoveries have immediate therapeutic implications, opening the door to more accurate diagnoses and individualized treatment plans. In the end, our study provides important insights for further investigation into ARDS and its treatment modalities



while laying the groundwork for experimental and clinical research in the future.

### Data availability statement

The original contributions presented in the study are included in the article/supplementary material. Further inquiries can be directed to the corresponding author.

### Ethics statement

The animal experimental processes were approved by the Ethics Committee of Hangzhou Hibio Technology Co., Ltd. (HB2311003). The study was conducted in accordance with the local legislation and institutional requirements.

### Author contributions

GL: Funding acquisition, Writing – original draft, Writing – review & editing. PG: Data curation, Formal analysis, Visualization, Writing – original draft, Writing – review & editing. KY: Conceptualization, Data curation, Formal analysis, Writing – original draft. WZ: Validation, Writing – original draft. HP: Validation, Writing – original draft.

### Funding

The author(s) declare that financial support was received for the research, authorship, and/or publication of this article. This study received support from the Zhejiang Provincial Traditional Chinese Medicine Science and Technology Plan Project (Grant No. 2024ZL528), under the supervision of GL.

## Conflict of interest

The authors declare that the research was conducted in the absence of any commercial or financial relationships that could be construed as a potential conflict of interest.

## Publisher's note

All claims expressed in this article are solely those of the authors and do not necessarily represent those of their affiliated

organizations, or those of the publisher, the editors and the reviewers. Any product that may be evaluated in this article, or claim that may be made by its manufacturer, is not guaranteed or endorsed by the publisher.

## Supplementary material

The Supplementary Material for this article can be found online at: <https://www.frontiersin.org/articles/10.3389/fimmu.2024.1365206/full#supplementary-material>

## References

- Matthay MA, Ware LB, Zimmerman GA. The acute respiratory distress syndrome. *J Clin Invest.* (2012) 122:2731–40. doi: 10.1172/jci60331
- Bos LDJ, Ware LB. Acute respiratory distress syndrome: causes, pathophysiology, and phenotypes. *Lancet.* (2022) 40010358:1145–56. doi: 10.1016/s0140-6736(22)01485-4
- Gorman EA, O'Kane CM, McAuley DF. Acute respiratory distress syndrome in adults: diagnosis, outcomes, long-term sequelae, and management. *Lancet.* (2022) 40010358:1157–70. doi: 10.1016/s0140-6736(22)01439-8
- Matthay MA, Zemans RL. The acute respiratory distress syndrome: pathogenesis and treatment. *Annu Rev Pathol.* (2011) 6:147–63. doi: 10.1146/annurev-pathol-011110-130158
- De Freitas Caires N, Gaudet A, Portier L, Tsicopoulos A, Mathieu D and Lassalle P. Endocan, sepsis, pneumonia, and acute respiratory distress syndrome. *Crit Care.* (2018) 22:1:280. doi: 10.1186/s13054-018-2222-7
- Pham T, Rubenfeld GD. Fifty years of research in ARDS. The epidemiology of acute respiratory distress syndrome. A 50th birthday review. *Am J Respir Crit Care Med.* (2017) 195:7860–70. doi: 10.1164/rccm.201609-1773CP
- Laffey JG, Bellani G, Pham T, Fan E, Madotto F, Bajwa EK, et al. Potentially modifiable factors contributing to outcome from acute respiratory distress syndrome: the LUNG SAFE study. *Intensive Care Med.* (2016) 42:12:1865–76. doi: 10.1007/s00134-016-4571-5
- Dang W, Tao Y, Xu X, Zhao H, Zou L, Li Y. The role of lung macrophages in acute respiratory distress syndrome. *Inflammation Res.* (2022) 71:12:1417–32. doi: 10.1007/s00011-022-01645-4
- Cannavò L, Perrone S, Viola V, Marseglia L, Di Rosa G, Gitto E. Oxidative stress and respiratory diseases in preterm newborns. *Int J Mol Sci.* (2021) 22(22):12504. doi: 10.3390/ijms222212504
- Sauler M, Bazan IS, Lee PJ. Cell death in the lung: the apoptosis-necroptosis axis. *Annu Rev Physiol.* (2019) 81:375–402. doi: 10.1146/annurev-physiol-020518-114320
- Cho SJ, Stout-Delgado HW. Aging and lung disease. *Annu Rev Physiol.* (2020) 82:433–59. doi: 10.1146/annurev-physiol-021119-034610
- Liu S, Fang X, Zhu R, Zhang J, Wang H, Lei J, et al. Role of endoplasmic reticulum autophagy in acute lung injury. *Front Immunol.* (2023) 14:1152336. doi: 10.3389/fimmu.2023.1152336
- Cai Y, Song W, Li J, Jing Y, Liang C, Zhang L, et al. The landscape of aging. *Sci China Life Sci.* (2022) 65:12:2354–454. doi: 10.1007/s11427-022-2161-3
- Childs BG, Durik M, Baker DJ, van Deursen JM. Cellular senescence in aging and age-related disease: from mechanisms to therapy. *Nat Med.* (2015) 21:12:1424–35. doi: 10.1038/nm.4000
- Rossiello F, Jurk D, Passos JF, d'Adda di Fagnana F. Telomere dysfunction in ageing and age-related diseases. *Nat Cell Biol.* (2022) 24:2:135–47. doi: 10.1038/s41556-022-00842-x
- Schumacher B, Pothof J, Vijg J, Hoeijmakers JHJ. The central role of DNA damage in the ageing process. *Nature.* (2021) 592:7856:695–703. doi: 10.1038/s41586-021-03307-7
- Verbeke EK, Caubergs M, Mertens I, Clement J, Lauweryns JM, Van de Woestijne KP. The senile lung. Comparison with normal and emphysematous lungs. I. Structural aspects. *Chest.* (1992) 101:3:793–9. doi: 10.1378/chest.101.3.793
- Al-Shaer MH, Choueiri NE, Correia ML, Sinkey CA, Barenz TA, Haynes WG. Effects of aging and atherosclerosis on endothelial and vascular smooth muscle function in humans. *Int J Cardiol.* (2006) 109:2:201–6. doi: 10.1016/j.ijcard.2005.06.002
- Ely EW, Wheeler AP, Thompson BT, Ancukiewicz M, Steinberg KP, Bernard GR. Recovery rate and prognosis in older persons who develop acute lung injury and the acute respiratory distress syndrome. *Ann Intern Med.* (2002) 136:1:25–36. doi: 10.7326/0003-4819-136-1-200201010-00007
- Clementi N, Ghosh S, De Santis M, Castelli M, Criscuolo E, Zanoni I, et al. Viral respiratory pathogens and lung injury. *Clin Microbiol Rev.* (2021) 34(3):e00103–20. doi: 10.1128/cmr.00103-20
- Schouten LR, van Kaam AH, Kohse F, Veltkamp F, Bos LD, de Beer FM, et al. Age-dependent differences in pulmonary host responses in ARDS: a prospective observational cohort study. *Ann Intensive Care.* (2019) 9:1:55. doi: 10.1186/s13613-019-0529-4
- Brandenberger C, Kling KM, Vital M, Christian M. The role of pulmonary and systemic immunosenescence in acute lung injury. *Aging Dis.* (2018) 9:4:553–65. doi: 10.14336/ad.2017.0902
- Voelkerding KV, Dames SA, Durtschi JD. Next-generation sequencing: from basic research to diagnostics. *Clin Chem.* (2009) 55:4:641–58. doi: 10.1373/clinchem.2008.112789
- Tacutu R, Thornton D, Johnson E, Budovsky A, Barardo D, Craig T, et al. Human Ageing Genomic Resources: new and updated databases. *Nucleic Acids Res.* (2018) 46:D1:D1083–d1090. doi: 10.1093/nar/gkx1042
- Ritchie ME, Phipson B, Wu D, Hu Y, Law CW, Shi W, et al. limma powers differential expression analyses for RNA-seq and microarray studies. *Nucleic Acids Res.* (2015) 43:7:e47. doi: 10.1093/nar/gkv007
- Szklarczyk D, Gable AL, Lyon D, Junge A, Wyder S, Huerta-Cepas J, et al. STRING v11: protein-protein association networks with increased coverage, supporting functional discovery in genome-wide experimental datasets. *Nucleic Acids Res.* (2019) 47:D1:D607–d613. doi: 10.1093/nar/gky1131
- Yu G, Wang LG, Han Y, He QY. clusterProfiler: an R package for comparing biological themes among gene clusters. *Omic.* (2012) 165:284–7. doi: 10.1089/omi.2011.0118
- Langfelder P, Horvath S. WGCNA: an R package for weighted correlation network analysis. *BMC Bioinf.* (2008) 9:559. doi: 10.1186/1471-2105-9-559
- Frost HR, Amos CI. Gene set selection via LASSO penalized regression (SLPR). *Nucleic Acids Res.* (2017) 45:12:e114. doi: 10.1093/nar/gkx291
- Li W, Yin Y, Quan X, Zhang H. Gene expression value prediction based on XGBoost algorithm. *Front Genet.* (2019) 10:1077. doi: 10.3389/fgene.2019.01077
- Yuan Y, Fu M, Li N, Ye M. Identification of immune infiltration and cuproptosis-related subgroups in Crohn's disease. *Front Immunol.* (2022) 13:1074271. doi: 10.3389/fimmu.2022.1074271
- Butler A, Hoffman P, Smibert P, Papalexi E, Satija R. Integrating single-cell transcriptomic data across different conditions, technologies, and species. *Nat Biotechnol.* (2018) 36:5:411–20. doi: 10.1038/nbt.4096
- Korsunsky I, Millard N, Fan J, Slowikowski K, Zhang F, Wei K, et al. Fast, sensitive and accurate integration of single-cell data with Harmony. *Nat Methods.* (2019) 16:12:1289–96. doi: 10.1038/s41592-019-0619-0
- Jin S, Guerrero-Juarez CF, Zhang L, Chang I, Ramos R, Kuan CH, et al. Inference and analysis of cell-cell communication using CellChat. *Nat Commun.* (2021) 12:1:1088. doi: 10.1038/s41467-021-21246-9
- Johnston CJ, Rubenfeld GD, Hudson LD. Effect of age on the development of ARDS in trauma patients. *Chest.* (2003) 124:2:653–9. doi: 10.1378/chest.124.2.653
- Meduri GU, Kohler G, Headley S, Tolley E, Stentz F, Postlethwaite A. Inflammatory cytokines in the BAL of patients with ARDS. Persistent elevation over time predicts poor outcome. *Chest.* (1995) 108:5:1303–14. doi: 10.1378/chest.108.5.1303
- Parcha V, Kalra R, Bhatt SP, Berra L, Arora G, Arora P. Trends and geographic variation in acute respiratory failure and ARDS mortality in the United States. *Chest.* (2021) 159:4:1460–72. doi: 10.1016/j.chest.2020.10.042

38. Jiang Y, Rosborough BR, Chen J, Das S, Kitsios GD, McVerry BJ, et al. Single cell RNA sequencing identifies an early monocyte gene signature in acute respiratory distress syndrome. *JCI Insight*. (2020) 5(13):e135678. doi: 10.1172/jci.insight.135678
39. Xiong S, Hong Z, Huang LS, Tsukasaki Y, Nepal S, Di A, et al. IL-1 $\beta$  suppression of VE-cadherin transcription underlies sepsis-induced inflammatory lung injury. *J Clin Invest*. (2020) 1307:3684–98. doi: 10.1172/jci.136908
40. Shive C, Pandiyan P. Inflammation, immune senescence, and dysregulated immune regulation in the elderly. *Front Aging*. (2022) 3:840827. doi: 10.3389/fragi.2022.840827
41. Palumbo S, Shin YJ, Ahmad K, Desai AA, Quijada H, Mohamed M, et al. Dysregulated Nox4 ubiquitination contributes to redox imbalance and age-related severity of acute lung injury. *Am J Physiol Lung Cell Mol Physiol*. (2017) 3123:L297–308. doi: 10.1152/ajplung.00305.2016
42. Martins R, Lithgow GJ, Link W. Long live FOXO: unraveling the role of FOXO proteins in aging and longevity. *Aging Cell*. (2016) 152:196–207. doi: 10.1111/acel.12427
43. Hong KU, Park YS, Seong YS, Kang D, Bae CD, Park J. Functional importance of the anaphase-promoting complex-Cdh1-mediated degradation of TMAP/CKAP2 in regulation of spindle function and cytokinesis. *Mol Cell Biol*. (2007) 2710:3667–81. doi: 10.1128/mcb.01386-06
44. Zhang S, Wang Y, Chen S, Li J. Silencing of cytoskeleton-associated protein 2 represses cell proliferation and induces cell cycle arrest and cell apoptosis in osteosarcoma cells. *BioMed Pharmacother*. (2018) 106:1396–403. doi: 10.1016/j.biopha.2018.07.104
45. Jin XX, Mei YN, Shen Z, Zhu JF, Xing SH, Yang HM, et al. A chalcone-syringaldehyde hybrid inhibits triple-negative breast cancer cell proliferation and migration by inhibiting CKAP2-mediated FAK and STAT3 phosphorylation. *Phytomedicine*. (2022) 101:154087. doi: 10.1016/j.phymed.2022.154087
46. Kim YW, Eom BW, Kook MC, Kim HS, Kim MK, Hwang HL, et al. Clinical implications of proliferation activity in T1 or T2 male gastric cancer patients. *Exp Mol Med*. (2015) 4711:e193. doi: 10.1038/emmm.2015.79
47. Avelar RA, Ortega JG, Tacutu R, Tyler EJ, Bennett D, Binetti P, et al. A multidimensional systems biology analysis of cellular senescence in aging and disease. *Genome Biol*. (2020) 211:91. doi: 10.1186/s13059-020-01990-9
48. Wu HL, Gong Y, Ji P, Xie YF, Jiang YZ, Liu GY. Targeting nucleotide metabolism: a promising approach to enhance cancer immunotherapy. *J Hematol Oncol*. (2022) 151:45. doi: 10.1186/s13045-022-01263-x
49. Chen Y, Zhang C, Jin S, Li J, Dai J, Zhang Z, et al. Pemetrexed induces ROS generation and cellular senescence by attenuating TS-mediated thymidylate metabolism to reverse gefitinib resistance in NSCLC. *J Cell Mol Med*. (2023) 2714:2032–44. doi: 10.1111/jcmm.17799
50. Huang X, Zhang X, Machireddy N, Evans CE, Trewartha SD, Hu G, et al. Endothelial FoxM1 reactivates aging-impaired endothelial regeneration for vascular repair and resolution of inflammatory lung injury. *Sci Transl Med*. (2023) 15709:eabm5755. doi: 10.1126/scitranslmed.abm5755
51. Varghese V, Magnani L, Harada-Shoji N, Mauri F, Szydlo RM, Yao S, et al. FOXM1 modulates 5-FU resistance in colorectal cancer through regulating TYMS expression. *Sci Rep*. (2019) 91:1505. doi: 10.1038/s41598-018-38017-0
52. Napoli JL. Cellular retinoid binding-proteins, CRBP, CRABP, FABP5: Effects on retinoid metabolism, function and related diseases. *Pharmacol Ther*. (2017) 173:19–33. doi: 10.1016/j.pharmthera.2017.01.004
53. Lee SA, Yang KJZ, Brun PJ, Silvaroli JA, Yuen JJ, Shmarakov I, et al. Retinol-binding protein 2 (RBP2) binds monoacylglycerols and modulates gut endocrine signaling and body weight. *Sci Adv*. (2020) 611:eaay8937. doi: 10.1126/sciadv.aay8937
54. McDonald KG, Leach MR, Brooke KWM, Wang C, Wheeler LW, Hanly EK, et al. Epithelial expression of the cytosolic retinoid chaperone cellular retinol binding protein II is essential for *in vivo* imprinting of local gut dendritic cells by luminal retinoids. *Am J Pathol*. (2012) 1803:984–97. doi: 10.1016/j.ajpath.2011.11.009
55. Jokela TA, Kärnä R, Makkonen KM, Laitinen JT, Tammi RH and Tammi MI. Extracellular UDP-glucose activates P2Y14 Receptor and Induces Signal Transducer and Activator of Transcription 3 (STAT3) Tyr705 phosphorylation and binding to hyaluronan synthase 2 (HAS2) promoter, stimulating hyaluronan synthesis of keratinocytes. *J Biol Chem*. (2014) 28926:18569–81. doi: 10.1074/jbc.M114.551804
56. Cho J, Yusuf R, Kook S, Attar E, Lee D, Park B, et al. Purinergic P2Y<sub>14</sub> receptor modulates stress-induced hematopoietic stem/progenitor cell senescence. *J Clin Invest*. (2014) 1247:3159–71. doi: 10.1172/jci61636
57. Müller T, Bayer H, Myrtek D, Ferrari D, Sorichter S, Ziegenhagen MW, et al. The P2Y14 receptor of airway epithelial cells: coupling to intracellular Ca<sup>2+</sup> and IL-8 secretion. *Am J Respir Cell Mol Biol*. (2005) 336:601–9. doi: 10.1165/ajrmb.2005-0181OC
58. Weiskopf D, Schmitz KS, Raadsen MP, Grifoni A, Okba NMA, Endeman H, et al. Phenotype and kinetics of SARS-CoV-2-specific T cells in COVID-19 patients with acute respiratory distress syndrome. *Sci Immunol*. (2020) 5(48):eabd2071. doi: 10.1126/sciimmunol.abd2071
59. Zhu G, Liu Y, Zhang W, Huang Y, Li K. CD27(+)/TIM-1(+) memory B cells promoted the development of Foxp3(+) Tregs and were associated with better survival in acute respiratory distress syndrome. *Immunol Res*. (2018) 662:281–7. doi: 10.1007/s12026-017-8983-2
60. Feng Z, Jing Z, Li Q, Chu L, Jiang Y, Zhang X, et al. Exosomal STIMATE derived from type II alveolar epithelial cells controls metabolic reprogramming of tissue-resident alveolar macrophages. *Theranostics*. (2023) 133:991–1009. doi: 10.7150/thno.82552
61. Oh WJ, Gu C. The role and mechanism-of-action of Sema3E and Plexin-D1 in vascular and neural development. *Semin Cell Dev Biol*. (2013) 243:156–62. doi: 10.1016/j.semcdb.2012.12.001